

# KODAIKANAL OBSERVATORY

BULLETIN Number 188

Solar Limb Gradient from Eclipse Spectra of  
February 15, 1961

\*Aleksandar Kubicela

## Abstract

On the occasion of the total solar eclipse of February 15, 1961 two spectrograms were obtained at the moments of second and third contact of the eclipse. The spectrograms contain a smooth transition of the photospheric spectrum into the chromospheric one and *vice versa*. Continual registration has been achieved by means of a moving plate combined with a slit spectrograph. The method adopted, and a description of the spectrograph and the chromospheric spectrophotometric results obtained have been published (Kubicela, 1968). In this study the 1961 eclipse data have been used to find the intensity of solar continuum radiation dependent on heliocentric heights within the last second of apparent solar radius.

## The observational material

For this purpose the spectrogram of the second contact has been chosen which is photometrically superior as was estimated from the analysis of the chromospheric spectrum. Because of lower speed of the photoplate, this spectrogram covers better the low intensity domain about the sensitivity threshold of the photoemulsion.

The spectrogram contains a well defined, 300Å wide, region of the spectrum about the H $\gamma$  line. The dispersion of the original negative is 12Å/mm. The scale in the direction perpendicular to the dispersion is such that 1 mm on the plate corresponds to 313 km on the sun in the radial direction.

The photometric calibration enables one to obtain monochromatic intensities in arbitrary units. The transformation into intensity values expressed in terms of intensity of the center of the solar disc has been realised indirectly.

The measured continuum wavelengths have been chosen satisfying the following conditions: 1) Microphotometric measurements on the spectrogram have to be made without interference with neighbouring spectral lines. The used portion of the continuum also has to be as free of absorption lines as possible in a high resolution spectrum, (Minnacrt et al 1940). This was done with the aid of the Utrecht Atlas. 2) The same wavelength intervals have to be free of chromospheric emission lines. The list of Mitchell (1947) aided such an examination.

In this way five wavelengths have been finally chosen. These are centered at  $\lambda_1=4215\text{\AA}$ ,  $\lambda_2=4316\text{\AA}$ ,  $\lambda_3=4336\text{\AA}$ ,  $\lambda_4=4419\text{\AA}$ , and  $\lambda_5=4477\text{\AA}$ .

Besides the already mentioned spectrograms there are 6 calibration spectra, obtained by a step slit fitted on after the eclipse to the same spectrograph and spectra taken in a similar way with different exposures, from 0<sup>s</sup>.05 to 1<sup>s</sup>.30. They were used in evaluating the calibration curve and the Schwarzschild exponent. In both cases previously obtained values (Kubicela 1968) have been confirmed.

---

\*On leave from Astronomical Observatory in Belgrade, Yugoslavia.

### Evaluation of the intensities

The second contact spectrogram and the calibration spectra were measured by the recording microphotometer of Kodaikanal Observatory. With a nearly square slit, 1 mm on each side, that corresponds to 0.5Å in the spectrum and 12.5 km height in the solar atmosphere for each of five wavelengths, two photometric scans have been traced in a direction perpendicular to the dispersion.

Before reduction to intensities, the photometric scans were smoothed to avoid fluctuations caused by running shadows prior to second contact. Along these smoothed profiles about 30 points, at 25 km intervals on the sun, have been measured.

In spite of somewhat larger errors which could be expected in the process of numerical differentiation, small intervals between neighbouring measured points were used in order to obtain better coverage of the intensity curve at the extreme solar limb. We minimize the scatter in the measured intensity values by scanning two independent profiles at each wavelength and taking a mean value of five intensity curves from the different wavelengths.

According to the procedure described earlier (Kubicela 1968) application of the calibration curve to photometric profiles gives observed intensities in arbitrary units. Afterwards, they have to be multiplied by the following factor

$$\frac{s}{s^p} = s^{1-p} \quad \dots (1)$$

Here  $s$  is the length on the plate from the measured point to the point where the extrapolated photographic density vanishes. Schwarzschild's exponent,  $p$ , was 0.70. The quantity  $s$  is proportional to the exposure time of the observed point of the photoplate. Thus, the denominator at the left side of the equation (1) represents the Schwarzschild correction. In this way the observed intensities along any of the photometric profiles have been related to a unit of time. At the same time, the quantity  $s$  is proportional to the interval of heights in the solar atmosphere which, at the observed instant, had not yet been occulted by the moon. The corrected intensities can be considered as intensities related to a unit of length along the solar radius. Then, the numerator of the left member of (1) converts these intensities into the integrated ones within the corresponding interval of the solar radius.

At this stage of the photometric procedure, it was found that it would be useful to have an independent control quantity to check the photometric transformations and especially the application of Schwarzschild's law. The 1961 observation does not have any control of this kind. However, in Appendix I such a procedure has been briefly proposed.

Further, the integrated intensities obtained from two photometric profiles have been separately averaged at each wavelength. The transformation to intensity distribution along the apparent solar radius,  $i_\lambda(h)$ , has been achieved by numerical differentiation. Due to small intervals between neighbouring measured points it was possible to use only the first differences of the integrated intensities.

In order to obtain a final mean value, the quantities  $i_{\lambda_1}(h) \dots i_{\lambda_5}(h)$  were multiplied with coefficients 3.155, 2.193, 1.560, 1.146 and 1.000 respectively. They were derived by satisfying the condition that all five curves  $i_{\lambda_i}(h)$ , after some distance from the limb, have the same level in arbitrary intensity units.

In this way we normalize the five curves on to one system to eliminate variation caused by instrumental sensitivity at the different wavelengths.

### The results

These "normalized intensities",  $I_{\lambda}$ , are presented in Table I. It contains,  $I_{\lambda}$  (columns 2 to 6), their mean values  $I_m$  in the same arbitrary units (column 7), natural logarithms of intensities  $I_m$  (column 8),  $I_m$  expressed in per cent of the central intensity of the solar disc (column 9) and corresponding heights in the solar atmosphere in km (column 10).

Table I

No.	$I_{4213}$	$I_{4310}$	$I_{4336}$	$I_{4413}$	$I_{4417}$	$I_m$	$\ln I_m$	$I_m$ (%)	$h$ (km)
1	2	3	4	5	6	7	8	9	10
1	4.3	2.1	6.1	4.0	1.4	3.6	1.283	1.9	+250
2	6.1	3.9	8.2	4.9	2.6	5.0	1.611	1.8	+225
3	6.3	6.1	5.8	6.5	3.8	5.7	1.741	2.0	+200
4	12.1	6.7	9.2	8.2	4.2	8.1	2.094	2.8	+175
5	6.6	8.0	10.9	9.4	6.1	8.2	2.105	2.9	+150
6	12.9	9.5	13.4	11.3	6.7	10.8	2.380	3.8	+125
7	12.6	10.0	16.6	15.2	9.1	12.5	2.525	4.4	+100
8	14.8	14.0	19.8	16.5	13.2	15.7	2.753	5.6	+ 75
9	21.8	19.6	23.0	16.5	15.2	19.2	2.960	6.8	+ 50
10	22.7	19.9	22.8	23.3	12.8	20.3	3.015	7.2	+ 25
11	24.6	26.0	23.7	25.2	17.7	23.4	3.152	8.3	0
12	29.3	26.5	28.0	26.3	21.2	26.4	3.278	9.4	- 25
13	32.5	33.8	34.0	30.9	22.8	31.2	3.443	11.1	- 50
14	35.6	32.8	32.1	28.7	24.4	30.7	3.430	10.9	- 75
15	38.5	35.8	34.2	32.1	27.7	33.7	3.510	12.0	-100
16	42.6	31.2	32.1	31.7	31.0	33.7	3.518	12.0	-125
17	34.7	39.0	44.8	29.8	30.4	35.7	3.578	12.7	-150
18	47.2	42.1	44.8	28.7	33.1	39.2	3.675	13.9	-175
19	47.0	46.8	44.8	32.1	36.9	41.5	3.729	14.7	-200
20	37.8	42.1	38.4	30.8	39.2	39.3	3.678	14.0	-225
21	41.0	35.8	53.3	42.2	38.4	42.1	3.743	15.0	-250
22	41.6	48.3	39.3	45.7	45.3	44.0	3.790	15.6	-275
23	41.0	49.9	41.3	51.5	44.6	45.7	3.826	16.2	-300
24	44.2	44.4	47.0	45.7	50.4	46.3	3.840	16.4	-325
25	47.2	48.3	51.5	45.9	43.7	47.3	3.860	16.8	-350
26	50.8	43.7	50.5	44.7	43.0	46.5	3.843	16.5	-375
27	47.2	48.0	44.2	48.1	40.2	45.5	3.822	16.2	-400
28	47.2	49.9	40.6		41.4	44.8	3.810	15.9	-425
29	59.8				45.5	52.6	3.968	18.6	-450
30	50.5				41.6	46.0	3.835	16.3	-475
31	47.6				45.4	46.5	3.843	16.5	-500
32	50.5					50.5	3.930	17.9	-525

The intensities  $I_m$  have also been shown in figure 1 by open circles, and the curve drawn through them as a heavy line. The abscissa contains the heights of column 10 of Table I, with the origin directly below the inflection-point of the intensity curve. The intensity scale on the left of the diagram is expressed in arbitrary units, and the one on the right expresses the intensity in per cent of the central intensity of the solar disc. In a typical eclipse observation, it is very difficult to establish the relation between these two scales. An usual method is the extrapolation of observations outside an eclipse (usually on a reliable intensity scale) to a region as close to the solar limb as possible. The same procedure has been

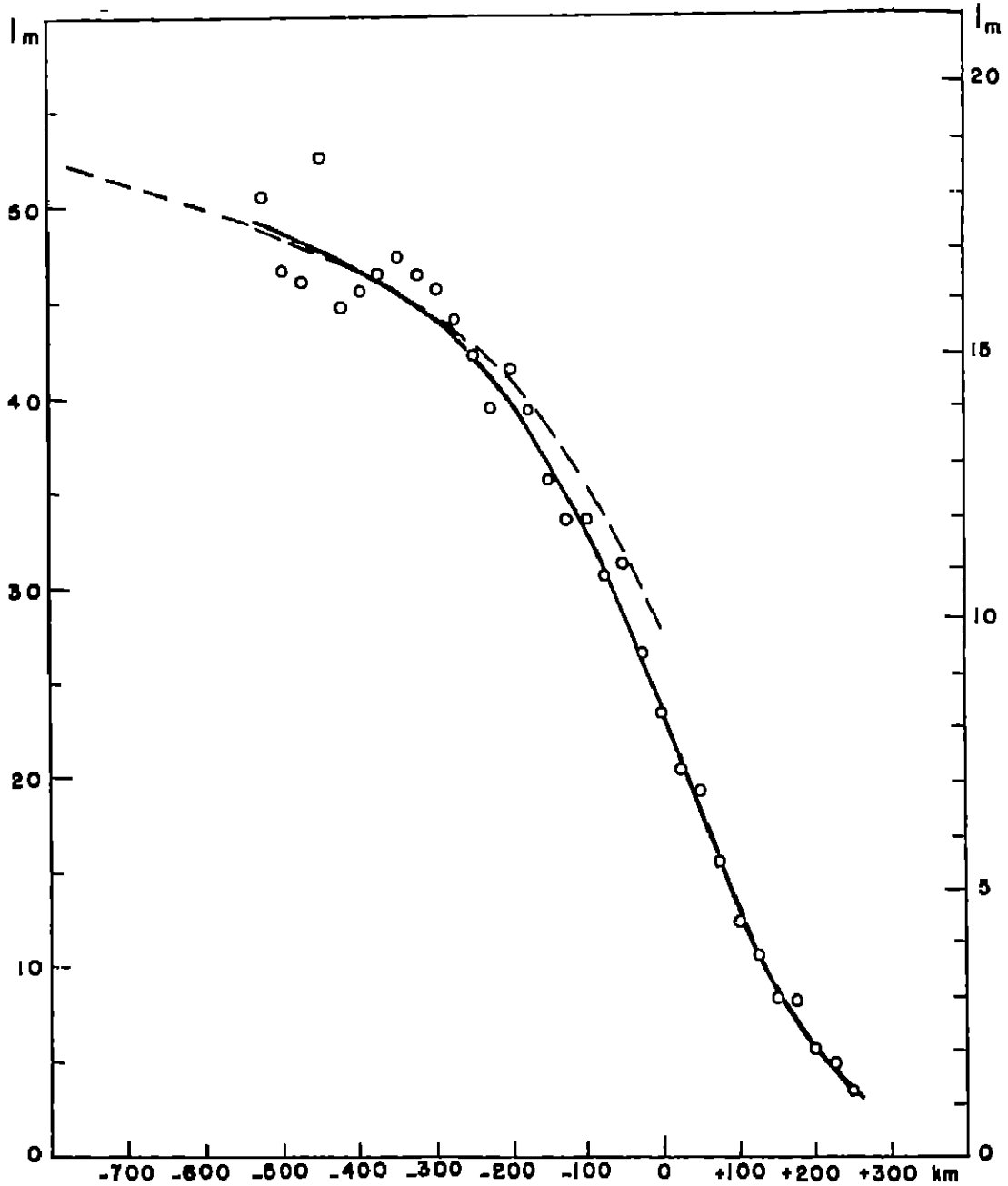


Figure 1

adopted here. The intensity curve (2) given by Pierce and Wadell (1961) was used. Hence

$$I(O, \theta) = a\lambda + b\lambda\mu + c\lambda [1 - \mu L_n(1 + \mu^{-1})] \dots (2)$$

Here  $\mu = \cos \theta$ , where  $\theta$  is the angle between the direction towards the observer and the radial direction at the observed point. The coefficients  $a\lambda$ ,  $b\lambda$ ,  $c\lambda$  are tabulated by Pierce and Wadell. We have in the present study interpolated these for a value of  $\lambda = 4350\text{\AA}$ . Equation (2) satisfies the observations with high accuracy within the interval  $0.2 \leq \mu \leq 1.0$ . We have extrapolated it until  $\mu = 0.003$ . This extrapolated curve of Pierce and Wadell to small values of  $\mu$  is shown in Figure 1 by the dashed curve.

A comparison of the observed curve with the extrapolated Pierce-Wadell curve within the height interval  $-200$  to  $-500$  km expresses the unit of our arbitrary intensity scale in per cent of central intensity of the solar disc. We thus find that one unit of the arbitrary scale equals  $0.355$  per cent of the intensity of the centre of the solar disc. The maximum deviation between the two curves occurs at the very limb and amounts to  $1.4$  per cent. An almost ideal agreement of the curves could be achieved by the translation of one of them for about  $35$  km along the abscissa and by the use of a coefficient  $0.348$  instead of  $0.355$ .

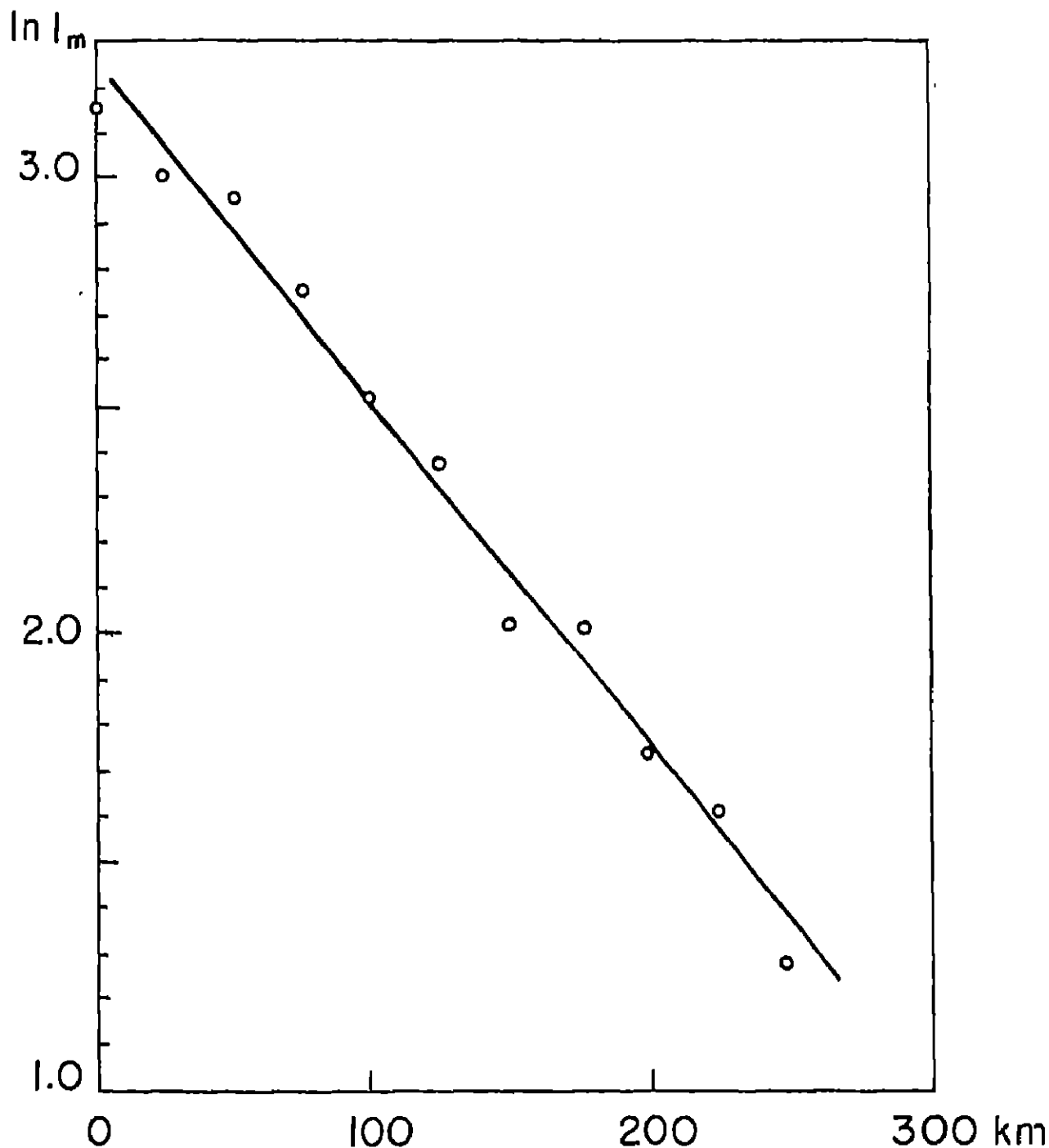


Figure 2

In figure 2, the natural logarithms of the intensity  $I_m$ , for  $h \geq 0$ , are shown. It can be seen that the curve, within the interval of positive heights satisfies the exponential expression

$$I = I_0 e^{-\gamma h} \quad \dots(3)$$

where the gradient  $\gamma = 7.4 \times 10^{-8} \text{ cm}^{-1}$ . Its reciprocal, the scale height,  $H$  is 135 km. The limb intensity  $I_0$ , amounts to 8.4 per cent of the intensity at the center of the solar disc.

With a rather high value of the scale height this observation joins some other similar observations (e.g. Lindblad and Kristenson, 1953). On the other hand, the theoretical values of  $H$ , under the assumption of hydrostatic equilibrium and temperature of about  $4500^\circ$ , are systematically lower:  $H = 54 \text{ km}$  (Minnaert, 1953) and  $H = 84 \text{ km}$  (Pagel, 1967). This discrepancy is, so far, unexplained.

#### Acknowledgement

This work was completed at the Kodaikanal Observatory and I wish to express my thanks to the institution for this opportunity. I am also deeply indebted to the Director, Dr. M. K. Vainu Bappu for his valuable advice on several occasions during the progress of the work.

Kodaikanal Observatory  
May 1969

#### REFERENCES

- Kubicla A, 1968, Publ. Astr. Obs. Beograd, 15
- Lindblad B., Kristenson H. 1953, Convegno di Scienze Fisiche Matematiche E Naturali, Roma, p. 61
- Minnaert M., Mulders G. P. W., Houtgast J., 1940, Photometric Atlas of the Solar Spectrum, Amsterdam.
- Minnaert M, 1953, The Sun (ed. Kuiper), Chicago, p. 88
- Mitchell S, 1947, Astrophys J. 105, p. 1
- Pagel B. E. J. 1967, Solar Physics (ed. Xanthakis), London, p. 11
- Pierce A. K., Wadell J. H. 1961, Mem. R. Ast. Soc., 68, p. 89.

## APPENDIX I

## The Control Photometric Field on a Moving Plate

It is useful to have a good control of photometric reductions when a moving photographic plate is used as the radiation receiver in an eclipse observation. In order to secure such a control, the following procedure can be used.

The region ABCD of a moving photoplate, P, Figure 1, is illuminated by an artificial light source. The field ABCD does not move with the plate. The illumination is uniform, it lasts for some time during which time it is constant, but

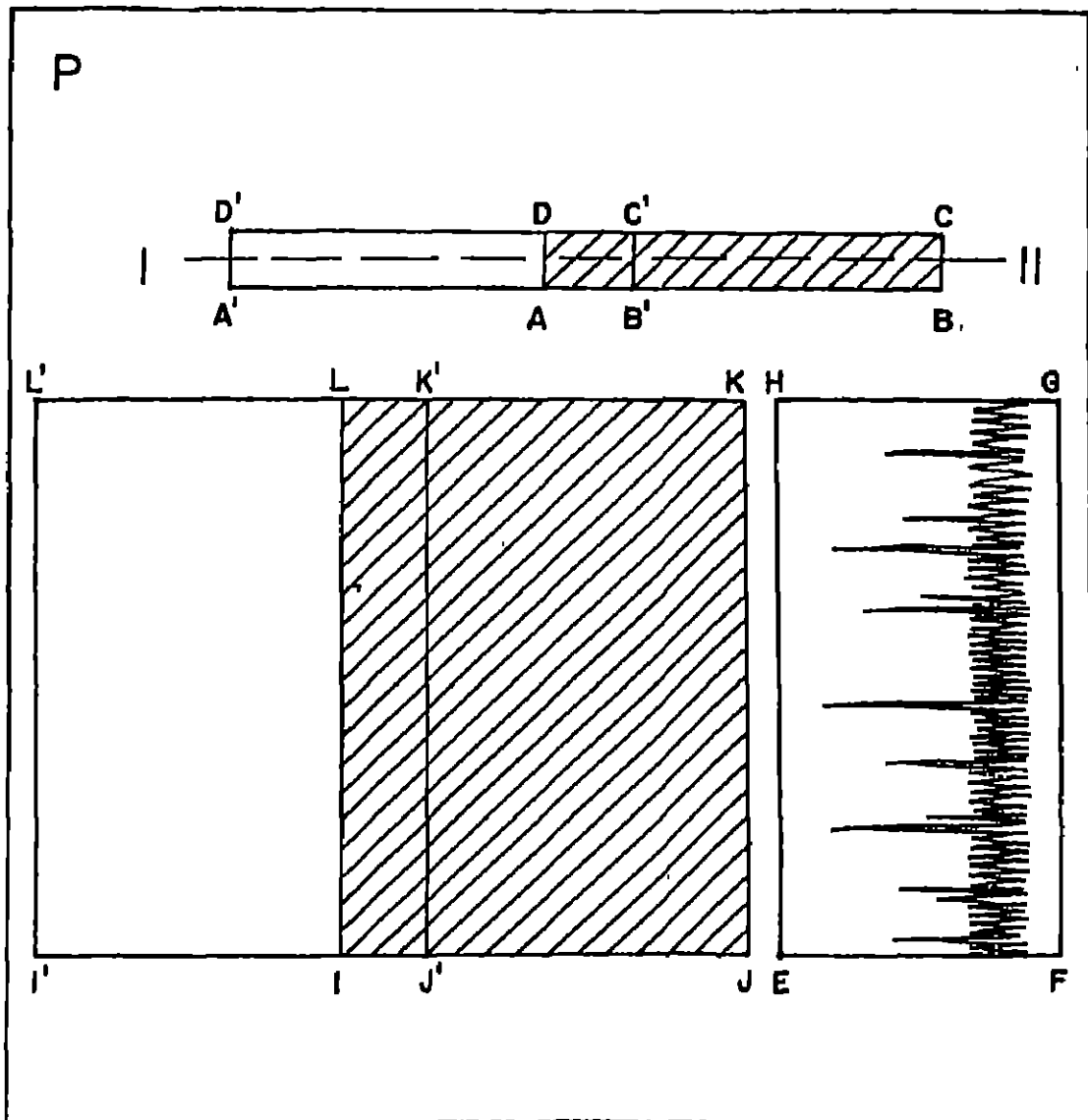


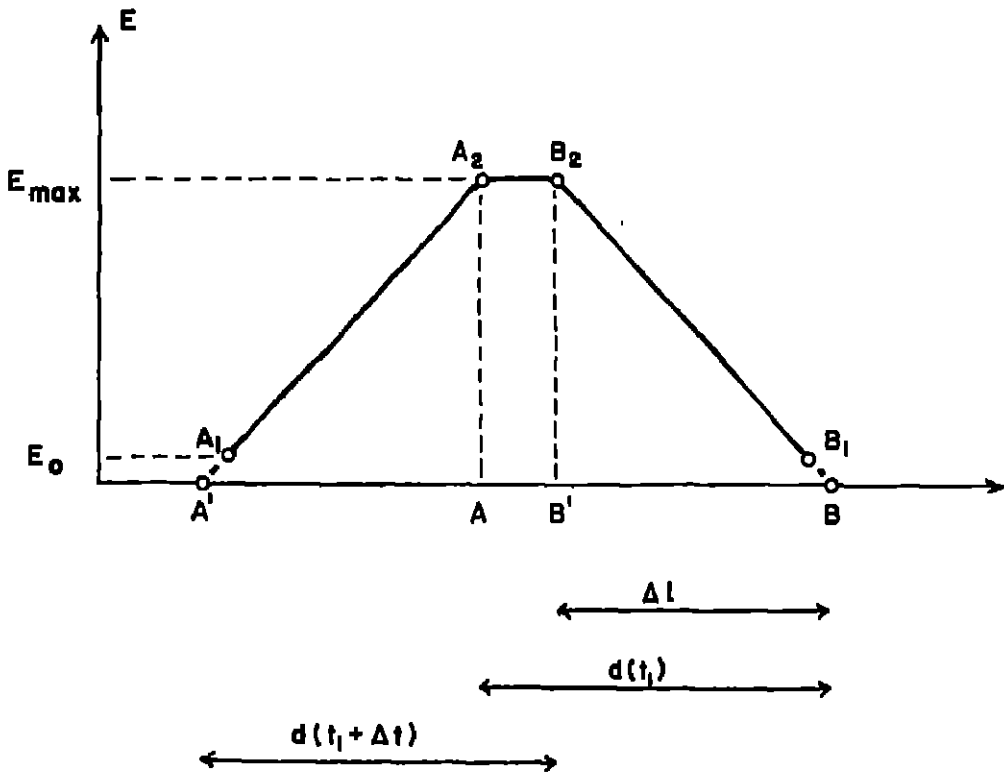
Figure 1.

starts and ends abruptly. The wavelengths of the radiation in the field are identical or similar to the wavelengths in the spectrum which are observed in the EFGH

regions of the plate. The length of the control field,  $d = \overline{AB}$ , is somewhat bigger than the total length,  $\overline{EF}$ , described by the plate during the movement. The intensity of light is such that the photographic density in the field ABCD nearly equals the expected density in the observed spectrum.

The desired illumination can be realized by a light source and an immovable mask with a window (of shape ABCD) immediately in front of the plate, or by a suitable projector inside the camera of the spectrograph.

The process is the following. The illumination of the field ABCD begins at the instant  $t_1$  after the plate has started moving and ends at the instant  $t_1 + \Delta t$  before the plate stops. In this way the plate is exposed to the radiation from the control field in the region  $A'BCD'$ . The distribution of the photographic density along the line I--II in Figure 1, is such that, after the correct application of the calibration curve and the Schwarzschild's law, the photometric profile must be like  $A_2A_2B_2B$  shown in Figure 2. Here the abscissa contains the lengths,  $l$ , in the direc-



tion of the movement of the plate. The ordinate represents the total radiant energy,  $E$ , that a surface element of the plate receives during the exposure interval between  $t_1$ , and  $t_1 + \Delta t$ .  $\Delta l$  is the distance covered by the plate within the interval  $\Delta t$ , and  $d(t_1)$  and  $d(t_1 + \Delta t)$  are the first and the last illuminated positions respectively of the field.

The energy  $E$  depends on the illumination,  $c$ , of the plate (the radiation energy received in a unit of time by a surface element of the plate in a given wavelength interval and of a given solid angle) according to



$$E = \int_{T_1}^{T_2} \epsilon dt. \quad \dots(1)$$

The limits of the integral (1),  $T_1$  and  $T_2$ , are the moments of the beginning and of the end of illumination of the observed element on the photographic plate. Because of constant illumination,  $E$  depends on time only through these limits.

Within the three sections of the profile in Figure 2, the limits of the integral (1) have the following values:

$$\begin{aligned} \text{On the section } \overline{A'A_2} : T_1 &= t \\ T_2 &= t_1 + t \end{aligned} \quad (2)$$

$$\begin{aligned} \text{On the section } \overline{A_2B_2} : T_1 &= t_1 \\ T_2 &= t_1 + t \end{aligned} \quad (3)$$

$$\begin{aligned} \text{On the section } \overline{B_2B} : T_1 &= t_1 \\ T_2 &= t. \end{aligned} \quad (4)$$

Here  $t$  is time connected with distances,  $l$ , on the plate by the equation of movement

$$l = v \cdot t + \text{const.} \quad (5)$$

where  $v$  is the constant speed of the plate with respect to the non-moving illuminated field.

From (1) and (2), and from (1) and (4), it can be seen that  $E$  is a linear function of time, and because of (5) it also depends linearly on  $l$ . The sections  $\overline{A'A_2}$  and  $\overline{B_2B}$  of the photometric profile are straight lines with the slope that reverses the sign when the variable moves from the lower to the upper limit of the integral (1). As both limits in (3) are constant, from (1) we find  $E = \text{const.} = E_{\text{max}}$ ; the section  $\overline{A_2B_2}$  in figure 3 is a straight line parallel to the abscissa.

The photometric control consists in comparison of the observed profile I-II, Figure 1, with the shape in Figure 2. The degree of agreement of corresponding sections of the observed profile with straight lines from Figure 2 is the measure of the attained accuracy in photometric transformations.

In practice, the small sections  $\overline{A'A}$ , and  $\overline{BB_1}$  of the profile in Figure 2 will be lost. It is a necessary consequence of the existence of the sensitivity threshold of a photoemulsion, but it does not prevent the application of the described procedure.

In the case of a sufficiently long spectrograph slit, where the length of its projection,  $d'$ , in the plane of the photoplate satisfies the condition  $d' \geq AB + EF$ ; alternatively, the photometric field can be realized by uniform illumination of a section of the slit itself. At the first instant this radiation forms a spectrum in the IJKL region of the plate. During the movement of the plate, on the surface I'JKL' a picture with photometric profiles analogous with the profile I-II, is being built. It is evident that such a photometric field can be analysed in each wavelength separately.

E R R A T A

KODAIKANAL OBSERVATORY BULLETIN No. 189

---

Location	Error	Corr.
Page A 164 -- Second line of abstract	displacements	displacements
Page A 164 - Sixth Line (ibid)	comparator	comparator

---